Water/fat separated Prostate Diffusion-Weighted Imaging using Dixon-encoded multi-shot EPI with structured low-rank reconstruction

Yiming Dong[1], David Atkinson[2], Kirsten Koolstra[3], Matthias J.P. van Osch[1], and Peter Börnert[1,4]
[1]C.J. Gorter MRI Center, Department of Radiology, LUMC, Leiden, Netherlands, [2]Centre for Medical Imaging, University College London, London, United Kingdom, [3]Philips, Best, Netherlands, [4]Philips Research Hamburg, Hamburg, Germany

Synopsis

Keywords: Prostate, Prostate

Motivation: Conventional single-shot EPI (ssh-EPI) is fast, but often causes geometric distortions, especially near the rectum.

Goal(s): In this research, a Dixon-msh-EPI technique is validated for prostate Diffusion-weighted Imaging (DWI).

Approach: Dixon-msh-EPI is proposed to reduce such distortions, while jointly separating water/fat components by a special structured low-rank reconstruction that also corrects shot-to-shot phase variations.

Results: Experiments were conducted on 7 healthy male volunteers using a 3T scanner comparing DW-ssh-EPI and Dixon-msh-EPI performance. The Dixon-msh showed significantly reduced geometric distortion and effective fat signal suppression, as scored by two readers. While both methods provided comparable image quality, Dixon-msh-EPI demonstrated improved motion-correction and geometric accuracy.

Impact: Dixon-msh-EPI offers improved prostate DWI by significantly reducing geometric distortions and enhancing across b-value registration. This technique could lead to more accurate diagnoses and has the potential to refine clinical MRI protocols, emphasizing precision in prostate diffusion imaging.

Introduction

Early detection and accurate characterization of prostate cancer are critical for effective treatment and thus improved patient outcomes[1,2]. Diffusion-weighted imaging (DWI) with ADC mapping could provide a non-invasive insight into the microstructure of prostate tissue[3], aiding in the diagnostic process. While single-shot EPI (ssh-EPI) is generally preferred for its speed in clinical prostate DWI, it is severely limited in image quality due to potential geometric distortions and T_2^* blurring[3]. Especially in the prostate, air/tissue susceptibility can vary significantly due to its close location to the rectum. Multi-shot EPI[3] (msh-EPI) can potentially address all these issues and provide higher spatial resolution, although it faces challenges with motion-induced shot-to-shot phase variations[4]. Moreover, in common with all EPI-based acquisitions, unsuppressed fat is a confounding factor due to the spatial displacements of fat signals, resulting from the chemical-shift effect[5,6].

To address these issues, we propose to use a Dixon-msh EPI acquisition combined with a structured low-rank reconstruction to simultaneously address shot-to-shot phase variations and the fat-suppression problem[7]. The DW Dixon-ms-EPI has notable advantages, including (1) effective phase-corrected averaging without fat-suppression pulse and measuring 2D-navigators[4]; (2) correction for residual geometric distortions using estimated B_0 map for free; (3) improved fat suppression; and (4) better "fat-based" image registration across b-values. In this study, we also evaluate Dixon-msh-EPI against standard fat-suppressed ssh-EPI for prostate DWI.

Methods

Dixon combined with msh-EPI (Dixon-ms-EPI) using structured low-rank reconstruction for DWI allows navigation-free joint estimation of water, fat and B_0 components. By applying two Hankel-matrix completions[8], the data redundancy along multi-shot/Dixon dimensions can be used to guide the reconstruction:

$$\{P_w, P_f\} = \underset{\tilde{x}_w, \tilde{x}_f \in \mathbb{C}^{Q\times N\times L}}{\operatorname{argmin}} \|AP - d\|_2^2 + \lambda_1 \|H(FP_w)\|_* + \lambda_2 \|H(FP_f)\|_*,$$

where $P = [P_w, P_f]^T = [\rho_{w,1,1}, \ldots, \rho_{w,N,1}, \ldots, \rho_{w,1,L}, \ldots, \rho_{w,N,L}, \rho_{f,1,1}, \ldots, \rho_{f,N,1}, \ldots, \rho_{f,1,L}, \ldots, \rho_{f,N,L}]^T$ represents the water/fat complex-valued images with L shots and N Dixon points, and A is the system matrix that enforces data consistency, H represents the Hankel-matrix transformation. There are also some advantages of doing Dixon for prostate DWI: after the reconstruction, residual geometric distortions can be further corrected using the Dixon B_0 fieldmap, with conjugate-phase reconstruction (CPR)[9] for free. Such B_0 map is estimated during reconstruction from the b=0 s/mm^2 data [5–7]. Separated fat signals can also be used for macroscopic motion tracking in DW Dixon-msh-EPI (Rigid + diffeomorphic field registrations were used in previous work[10]), and fat can be suppressed over the complete multi-peak fat spectrum[6,11].

Experiments were conducted using a 3T scanner on 7 healthy male volunteers who provided informed consent. They underwent a standard prostate 2D-T2w-TSE scan, followed by two baseline DWI scans and a few additional scans. Detailed scan parameters for these sequences are presented in Table 1 (A). Reconstruction utilizing SENSE for the ssh-EPI was compared to the structured low-rank for the Dixon 3-shot EPI. CPR was not used in this comparison.

The comparative analysis involved evaluating ADC values, which were obtained using a mono-exponential model in ROIs placed in the transition zone areas while being free of susceptibility-related artifacts. Statistical significance was tested using a paired Wilcoxon test. Two expert readers assessed image quality from both DWI protocols using a 5-point Likert scale[12]. Criteria included geometric distortion, prostate edge clarity, perceived SNR, and overall image quality.

Results

Dixon-ms-EPI showed less geometric distortion than ssh-EPI as scored by both readers; however, only reader 2 perceived the SNR of ssh-EPI to be significantly higher than Dixon-ms-EPI, as shown in Table 1(B). Figure 1 shows a slice illustrating the reduced geometric distortion of Dixon-msh-EPI versus ssh-EPI, compared to the T2w-TSE reference image. It is also evident that the CPR + B_0 map can further correct the remaining geometric distortions. In Figure 2, Dixon ssh-EPI effectively suppressed fat signals, unlike fat-suppressed SPAIR[13] ssh-EPI, which failed in this chosen case. In Figure 3, the prostate scan exhibited motion-induced deformities in the water-registered images, which can be much better registered using fat images. Figure 4 shows comparable ADC values between Dixon-ssh-EPI and ssh-EPI (top table), but ssh-EPI had certain regions with noticeable ADC mapping degradation (bottom).

Discussion and conclusion

This study confirmed that Dixon-msh-EPI outperforms ssh-EPI with regard to reduced geometric distortions, whereas other factors of overall image quality were comparable. Note that scan time was kept constant. The inherent ability of Dixon-msh-EPI to access fat information can aid in motion correction by applying more robust fat-based registration. Dixon-msh-EPI also allowed a further reduction in geometric distortion by exploiting the jointly estimated B_0 map, and showed its effectiveness in fat suppression. Therefore, it presents a valuable alternative to fat-suppressed ssh-EPI. In addition, eliminating the SPAIR pulse saved 130 ms per shot, which improved scan efficiency. Notably, this initial study was based on healthy volunteers, further clinical studies with patients are needed to understand its diagnostic efficacy.

Acknowledgements

The authors would like to acknowledge NWO-TTW (HTSM-17104).

References

1. Hoeks CMA, Barentsz JO, Hambrock T, et al. Prostate cancer: Multiparametric MR imaging for detection, localization, and staging. Radiology. 2011;261(1).

2. Giganti F, Kirkham A, Kasivisvanathan V, et al. Understanding PI-QUAL for prostate MRI quality: a practical primer for radiologists. Insights Imaging. 2021;12(1).

3. Tamada T, Kido A, Ueda Y, et al. Comparison of single-shot EPI and multi-shot EPI in prostate DWI at 3.0 T. Sci Rep. 2022;12(1):1-10.

4. Jeong HK, Gore JC, Anderson AW. High-resolution human diffusion tensor imaging using 2-D navigated multishot SENSE EPI at 7 T. Magn Reson Med. 2013;69(3):793-802. doi:10.1002/mrm.24320 5. Dong Y, Riedel M, Koolstra K, van Osch MJP, Börnert P. Water/fat separation for self-navigated diffusion-weighted multishot echo-planar imaging. NMR Biomed. 2023;36(1):e4822.

6. Dong Y, Koolstra K, Riedel M, van Osch MJP, Börnert P. Regularized joint water–fat separation with B0 map estimation in image space for 2D-navigated interleaved EPI based diffusion MRI. Magn Reson Med. 2021;86(6):3034-3051.

7. Dong Y, Koolstra K, Li Z, Riedel M, Osch MJP van, Börnert P. Structured low-rank reconstruction for navigator-free water/fat separated multi-shot diffusion-weighted EPI. Magn Reson Med. Published online September 27, 2023.

8. Mani M, Jacob M, Kelley D, Magnotta V. Multi-shot sensitivity-encoded diffusion data recovery using structured low-rank matrix completion (MUSSELS). Magn Reson Med. 2017;78(2):494-507.

9. Man LC, Pauly JM, Macovski A. Multifrequency interpolation for fast off-resonance correction. Magn Reson Med. 1997;37(5):785-792.

10. Garyfallidis E, Brett M, Amirbekian B, et al. Dipy, a library for the analysis of diffusion MRI data. Front Neuroinform. 2014;8(FEB).

11. Ren J, Sherry AD, Malloy CR. 1H MRS of intramyocellular lipids in soleus muscle at 7 T: Spectral simplification by using long echo times without water suppression. Magn Reson Med. 2010;64(3):662-671.

12. Stocker D, Manoliu A, Becker AS, et al. Image Quality and Geometric Distortion of Modern Diffusion-Weighted Imaging Sequences in Magnetic Resonance Imaging of the Prostate. Invest Radiol. 2018;53(4):200-206.

13. Udayasankar UK, Martin D, Lauenstein T, et al. Role of spectral presaturation attenuated inversion-recovery fat-suppressed T2-weighted MR imaging in active inflammatory bowel disease. Journal of Magnetic Resonance Imaging. 2008;28(5):1133-1140.

Figures

Table 1. (A) sequence parameters, and (B) Qualitative comparison between DW-Dixon-3shot-EPI and ssh-EPI. In total 92 slices were evaluated by two readers based on various scoring criteria. There was significantly less geometric distortion in Dixon-3shot-EPI compared to ssh-EPI evaluated by both readers (P<0.05). Reader 2 scored the perceived SNR of ssh-EPI significantly higher than that of Dixon-3shot-EPI (P<0.05), whereas there was no significant difference in the first reader's report (P>0.05). There was no significant difference in all other aspects (P>0.05).

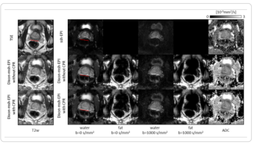

Figure 1. Comparison of ssh-EPI, Dixon-msh-EPI (with and without CPR) results for one slice of a volunteer. The left column shows T2w TSE images for reference, and Dixon-msh-EPI water/fat merged b=0 s/mm^2 image which may offer a different fat-present contrast. The right column shows the three techniques and their ADC maps. Using SPAIR means: no fat images for ssh-EPI. The increased bandwidth in Dixon-msh-EPI's reduces geometric distortions, and its B_0 map helps to further correct distortion via CPR. Red lines on T2w TSE highlight geometric distortions on water DWIs (b=0 s/mm^2).

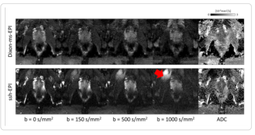

Figure 2. Comparison between Dixon-msh-EPI and SPAIR-ssh-EPI for fat suppression in a single subject. While SPAIR is commonly used in prostate DWI for fat suppression, it failed in this measurement, showing undiffused but unsuppressed fat signals (red arrow). In contrast, Dixon-msh EPI effectively suppressed them. If unsuppressed fat signals are superimposed on the prostate in routine scans, remeasurement may be required, e.g., by retuning the shimming or changing the SENSE factor. In practice, immediate correction during clinical sessions is challenging and time-consuming.

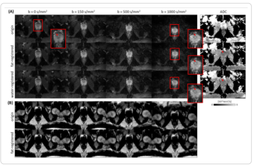

Figure 3: Gross motion and b-value based correction. Subjects were instructed to move between b-value acquisitions, resulting in spatial discrepancies. A slice displayed from a subject's prostate over 4 b-values, (A) shows water DWI, and (B) shows fat DWI. The top of (A) shows the original data and its ADC map. Two registration methods follow: using fat (fat-registered) and water images (water-registered). When fat images are used for registration, the structure aligns well (red arrows and zoomed areas). However, direct water registration can distort structures and blur ADC maps.

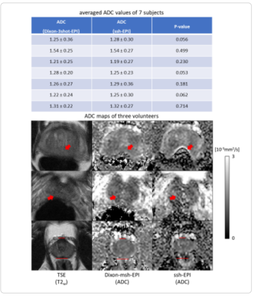

Figure 4: ADC mapping. (top table) Mean ADC values from 6 slices for each technique, showed no significant difference. (bottom Figure) Prostate T2w TSE images and ADC maps from Dixon-msh-EPI and ssh-EPI of three volunteers. In the first volunteer, ssh-EPI shows signal pile-up leading to erroneous ADC values (red arrows) whereas Dixon-msh-EPI reduces such artifacts. In the second, Dixon-msh-EPI reduces susceptibility artifacts (red arrows) and provides stable ADC mapping. In the third case, Dixon-msh-EPI better matches the TSE image in prostate position and shape (red bars).